PLOS ONE

RESEARCH ARTICLE

Antioxidant properties of bee propolis and an important component, galangin, described by X-ray crystal structure, DFT-D and hydrodynamic voltammetry

Francesco Caruso ⓘ, Molly Berinato, Melissa Hernandez, Stuart Belli, Christopher Smart, Miriam Rossi *

Department of Chemistry, Vassar College, Poughkeepsie, New York, United States of America

* Rossi@vassar.edu

Abstract

Propolis is produced by honeybees and used to seal their hives for defensive purposes and has been used in ethnopharmacology since ancient times. It is a lipophilic material containing a large collection of naturally produced plant organic molecules, including flavonoids. The flavonoid galangin is consistently found in propolis, independent of the hive geographical location and its X-ray crystal and molecular structure is reported. The antioxidant scavenging of superoxide by galangin and propolis is here presented. Using a cyclic voltammetry technique developed in our lab, we show that galangin is an excellent scavenger of the superoxide radical, perhaps even better than quercetin. Our results show that galangin displays a Superoxide Dismutase (SOD) function. This is described experimentally and theoretically (DFT). Two modes of scavenging superoxide are seen for galangin: (1) superoxide radical extraction of H atom from the hydroxyl moieties located in position 3 and 5 of galangin, which are also associated with proton incorporation defining the SOD action; (2) π-π interaction among several superoxide radicals and the galangin polyphenol ring that evolve towards release of O_2 and H_2O_2. We describe these two actions separately as their relative sequence, and/or combination, cannot be defined; all these processes are thermodynamically spontaneous, or subjected to mild barriers.

Introduction

Bee propolis is a viscous natural product produced by honeybees to seal their hive. Although its chemical composition varies according to environmental conditions, geographical location and available plant populations, the biological health benefits of propolis long have been appreciated throughout the world as part of traditional medicines. For instance, ancient Egyptians used propolis in embalming procedures because of its antimicrobial properties [1, 2]. The extensive health properties arise from the compounds in propolis. Notwithstanding the variations described earlier, bee propolis consistently contains a high concentration of phenolic

compounds, including flavones. In a recent study, galangin and chrysin were determined to be the most abundant polyphenols of a brown propolis extract [3]. Galangin, 3,5,7-trihydroxyflavone, is recognized to have significant beneficial biological activities such as anticancer [4, 5], antioxidant [6, 7]. Galangin is also found in plants such as *Alpinia officinarum* Hance (Zingiberaceae), or lesser galangal, and has been used as a spice and in herbal remedies for a variety of ailments in Ayurvedic and Chinese medicine for centuries [8, 9].

In this work, we have studied the antioxidant activity of galangin and of samples of bee propolis from Wappingers Falls in the Mid-Hudson region of New York State, USA, using the Rotating Ring Disk Electrode (RRDE) cyclic voltammetry technique that was developed in our laboratory. This method permits us to evaluate the superoxide radical scavenging activity of the pure compound, galangin, as well as samples of bee propolis. Additionally, we obtained high quality crystals of galangin, suitable for X-ray diffraction studies and we describe the molecular geometry and intermolecular interactions. Earlier structure-activity studies have suggested that the 2,3-double bond in conjugation with the 4-oxo group in the flavonoid structure is a major determinant of flavonoid antioxidant activity in mitochondria [10]. Many studies relating to flavonoid and polyphenolic antioxidant potential have been reported [11–18]. In our study, we focus on the slight structural differences between galangin and chrysin, as they can be related to the experimental determination of superoxide scavenging. Moreover, using computational results from dispersion-corrected Density Functional Theory (DFT-D), we study interactions among galangin and superoxide radicals. We suggest a mechanism for scavenging of the superoxide radical anion by galangin, and bee propolis, in agreement with our cyclovoltammetry findings.

Experimental section

X-ray.   Galangin (Indofine Chemical Co, Hillsborough, NJ, USA) was recrystallized from ethanol by slow evaporation. Table 1 shows the crystal data. Data collection was taken with a Bruker Smart APEXII single crystal X-ray diffractometer, with a Charge Coupled Device Detector and the experiment was done at 125 K using a cold liquid nitrogen stream from Oxford cryosystems. The X-ray source emitted $Mo_{K\alpha}$ radiation at 0.71073 Å. We used the SHELX program to determine and refine antioxidant crystal structure [19], and input the X-ray data into the MERCURY program to produce images of the molecules and crystal packing [20]. Crystal data of galangin have been deposited at the Cambridge Structural Database (CSD) and are available at https://www.ccdc.cam.ac.uk/structures/? using Identifier CCDC number 2123390.

RRDE measurement of antioxidant activity.   Materials used to determine the antioxidant activity of galangin and propolis were tetrabutylammonium bromide (TBAB; Sigma Aldrich) and 99% anhydrous Dimethyl Sulfoxide (DMSO; Sigma Aldrich. Galangin (Indofine Chemical Co., Hillsborough, NJ, USA). Propolis was provided by a co-author (C. Smart), from his own hive in the Hudson Valley. The 0.1 M TBAB/DMSO solution was used to produce electric current and enhance the occurrence of redox reactions. Antioxidant activity was measured via the hydrodynamic voltammetry technique with a rotating ring disk electrode (RRDE). The equipment used in this experiment was an MSR electrode rotator with CE and ETL marks, together with a WaveDriver 20 benchtop USB from Pine Instrumentation. The main electrode tip was an E6RI ChangeDisk with a rigid gold ring and gold disk (Au/Au) insert. Before and after each experiment, 0.3μL Alumina suspension was used to clean the disk electrode tip (Allied High Tech Products, Inc, Rancho Dominguez, CA, USA) on a moistened polishing microcloth to eliminate potential film formation. A Platinum (Pt) reference electrode and Pt counter electrode were also used in this experiment. All electrodes were obtained from Pine Research

Table 1. Crystal data of galangin●H$_2$O.

Empirical formula	C$_{15}$ H$_{10}$ O$_5$ ·H$_2$O	
Formula weight	280.25	
Temperature	125(2) K	
Wavelength	0.71073 Å	
Crystal system	Triclinic	
Space group	P-1	
	a = 3.8308(13) Å	α = 80.139(4°.
	b = 11.080(4) Å	β = 86.049(4°.
	c = 14.741(5) Å	γ = 83.351(4°.
Volume	611.5(4) Å3	
Z	2	
Density (calculated)	1.522 Mg/m3	
Absorption coefficient	0.117 mm-1	
F(000)	292	
Crystal size	0.23 x 0.19 x 0.05 mm3	
Theta range for data collection	1.40 to 27.48°.	
Index ranges	-4<=h<=4, -14<=k<=14, -19<=l<=19	
Reflections collected	7372	
Independent reflections	2769 [R(int) = 0.0259]	
Completeness to theta = 27.48°	99.6%	
Absorption correction	Empirical	
Max. and min. transmission	0.9942 and 0.9735	
Refinement method	Full-matrix least-squares on F2	
Data / restraints / parameters	2769 / 0 / 238	
Goodness-of-fit on F2	0.972	
Final R indices [I>2sigma(I)]	R1 = 0.0364, wR2 = 0.0993	
R indices (all data)	R1 = 0.0454, wR2 = 0.1066	
Largest diff. peak and hole	0.335 and -0.213 e.Å-3	

https://doi.org/10.1371/journal.pone.0267624.t001

Durham, NC, USA. [21]. Cyclic voltammagrams were run using a Solartron SI 1287 Potentio-stat/galvanostat (Solartron Analytical, Oakridge, TN, USA) controlled through Coreware© software.

The antioxidant activity of galangin was determined based on its superoxide radical scavenging ability that was measured using the protocol developed in our lab [22]. A stock solution of galangin, 0.02 M, in anhydrous DMSO was used in trials, whereas 0.335 g of propolis were dissolved in 10 ml of DMSO and used as stock solution. For the experiment, the electrolytic cell was bubbled for 5 minutes with a dry O$_2$/N$_2$ (35%/65%) gas mixture to establish its dissolved oxygen level. The Au disk electrode was then rotated at 1000 rpm while the disk was swept from 0.2 V to -1.2 Volts and the ring was held constant at 0.0 Volts, the disk voltage sweep rate was set to 25 mV/s. In summary, 4 runs plus blank were performed in the RRDE experiment for galangin to determine the antioxidant activity with equal addition of 5 μL of galangin stock solution, whereas 5 aliquots, were added for propolis study.

Results from each run were collected on Aftermath software and represented as voltammograms showing current vs. potential graphs that were later analyzed using Microsoft Excel. In an RRDE voltammetry experiment, the generation of the superoxide radicals occurs at the disk

electrode while the oxidation of the residual superoxide radicals (that have not been scavenged by the scavenger) occurs at the ring electrode.

Reaction 1: Reduction of molecular oxygen at disk electrode

$$\text{Disk current} \quad O_2 + e\text{-} \rightleftharpoons O_2 \bullet^- \tag{1}$$

Reverse Reaction 2: Oxidation of superoxide radicals at the ring

$$\text{Ring current} \quad O_2 \bullet^- \rightleftharpoons O_2 + e\text{-} \tag{2}$$
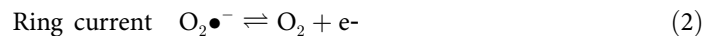
Thus, the rate at which increasing concentrations of galangin scavenged the generated superoxide radicals during the electrolytic reaction was determined by obtaining the quotient of the ring current and the disk current (percent value) at each concentration. These values were denoted as the *collection efficiency* of the scavenger at different concentrations. Using Microsoft Excel, collective efficiency values were plotted against the corresponding concentrations of galangin to produce a graph illustrating the effect of increasing concentrations of galangin on the scavenging of superoxide radicals in the electrolytic solution. Ultimately, the slope of the curves served as a quantitative measure of the antioxidant activity of galangin and propolis.

Computational experiments. Antioxidant activity of galangin studied using DFT. Calculations were performed using programs from Biovia (SanDiego, CA, USA). Density functional theory (DFT) code DMol3 was applied to calculate energy, geometry, TS and frequencies implemented in Materials Studio 7.0 [23]. We employed the double numerical polarized (DNP) basis set that included all the occupied atomic orbitals plus a second set of valence atomic orbitals, and polarized d-valence orbitals [24]; the correlation generalized gradient approximation (GGA) was applied including Becke exchange [25], plus BLYP-D correlation including Grimme's correction when van der Waals interactions were involved [26]. We used the DNP basis set, which consists of a double-numeric quality basis set for approximately 2 atomic orbitals for each one occupied in free atom (DN), plus basis with polarization functions, that is, functions with angular momentum one higher than that of highest occupied orbital in free atom.

Calculations were performed with DMSO solvent inclusion, using the continuous model of Dmol³ [27]. We used the DNP basis set, which consists in a double-numeric quality basis set for approximately 2 atomic orbitals for each one occupied in free atom (DN) plus basis with polarization functions, that is, functions with angular momentum one higher than that of highest occupied orbital in free atom. All electrons were treated explicitly and the real space cutoff of 5 Å was imposed for numerical integration of the Hamiltonian matrix elements. The self-consistent field convergence criterion was set to the root mean square change in the electronic density to be less than 10^{-6} electron/Å^3.

No human, animal or cell studies were used in research described in this manuscript.

Results and discussion

X-ray study

The galangin crystal grown after a few days from an ethanol solution showed color variation: it was clear when observed in one direction but reddish-yellow when observed at an approximate perpendicular direction. A data crystal was chosen (Fig 1) and an APEX2 DUO platform X-ray diffractometer from Bruker Advanced X-ray Solutions was used to obtain X-ray data measurements at 125 K. The crystal structure was solved and refined using ShelX programs [19]. Views of the crystal structure down the crystallographic axes, *a*, *b* and *c* are shown in S1 Fig. Torsion angles show the chromone moiety rings, A and C in Fig 2A, are in the same plane, while the
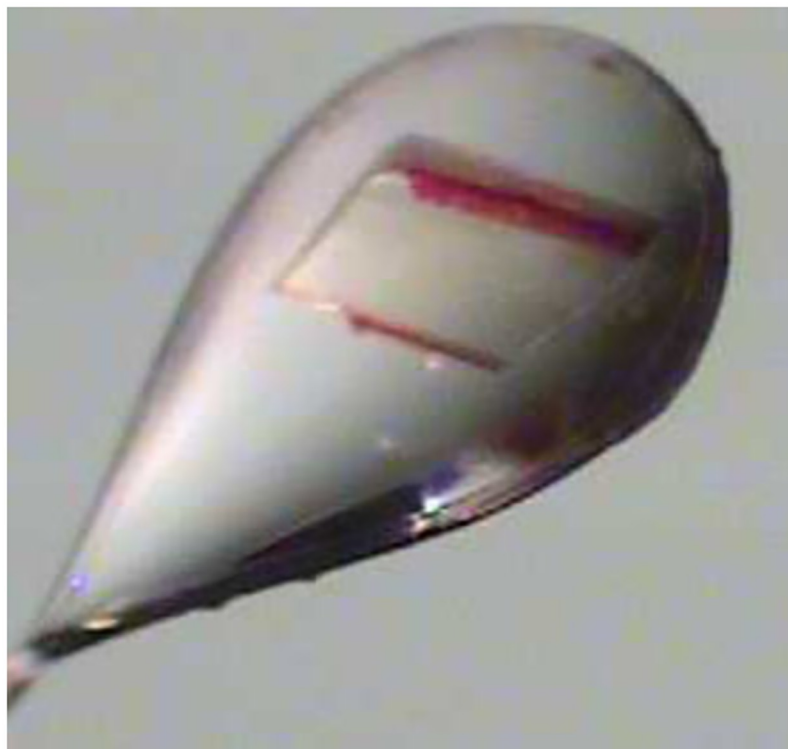
Fig 1. Galangin data crystal showing the color variation.

phenyl ring, designated B, is rotated -45.1(2˚ degrees off that plane. An analysis of 852 flavone structures in the CCSD shows that this value is uncommon (the mean torsion angle value is -11˚) [28].

Although galangin was crystallized from ethanol, a water molecule is present in the asymmetric unit. The water molecules function as hydrogen bonded bridges between layers of galangin molecules. Additionally, the distance between water oxygen atoms (viewed down the *a*-axis) is equal to the crystallographic *a*-axis (Fig 2B). The hydrogen bond parameters are listed in Table 2 and shown in Fig 2C. Besides these strong interactions, the crystal structure of galangin highlights the strong offset stacking between layers of galangin molecules (S2 Fig).

The results from our experimental RRDE studies show that galangin has very strong antioxidant activity (described later) towards the superoxide radical anion and are compatible with earlier work using the DPPH method to evaluate galangin radical scavenging ability [29]. The galangin crystal structure with its rich network of hydrogen bonds and stacking interactions supports this conclusion. We then sought to explain this strong antioxidant behavior by using computational methods to explore galangin scavenging behavior with the superoxide radical anion.

Antioxidant activity of galangin studied using DFT

Galangin X-ray coordinates were input into Materials Studio program DMOL^3, and Fig 3A shows relevant distances obtained after geometry optimization. This structure was obtained as an energy minimum, i.e. having only positive frequencies after vibrational analysis calculation; these distances will be of interest for comparison with the structural changes occurring after
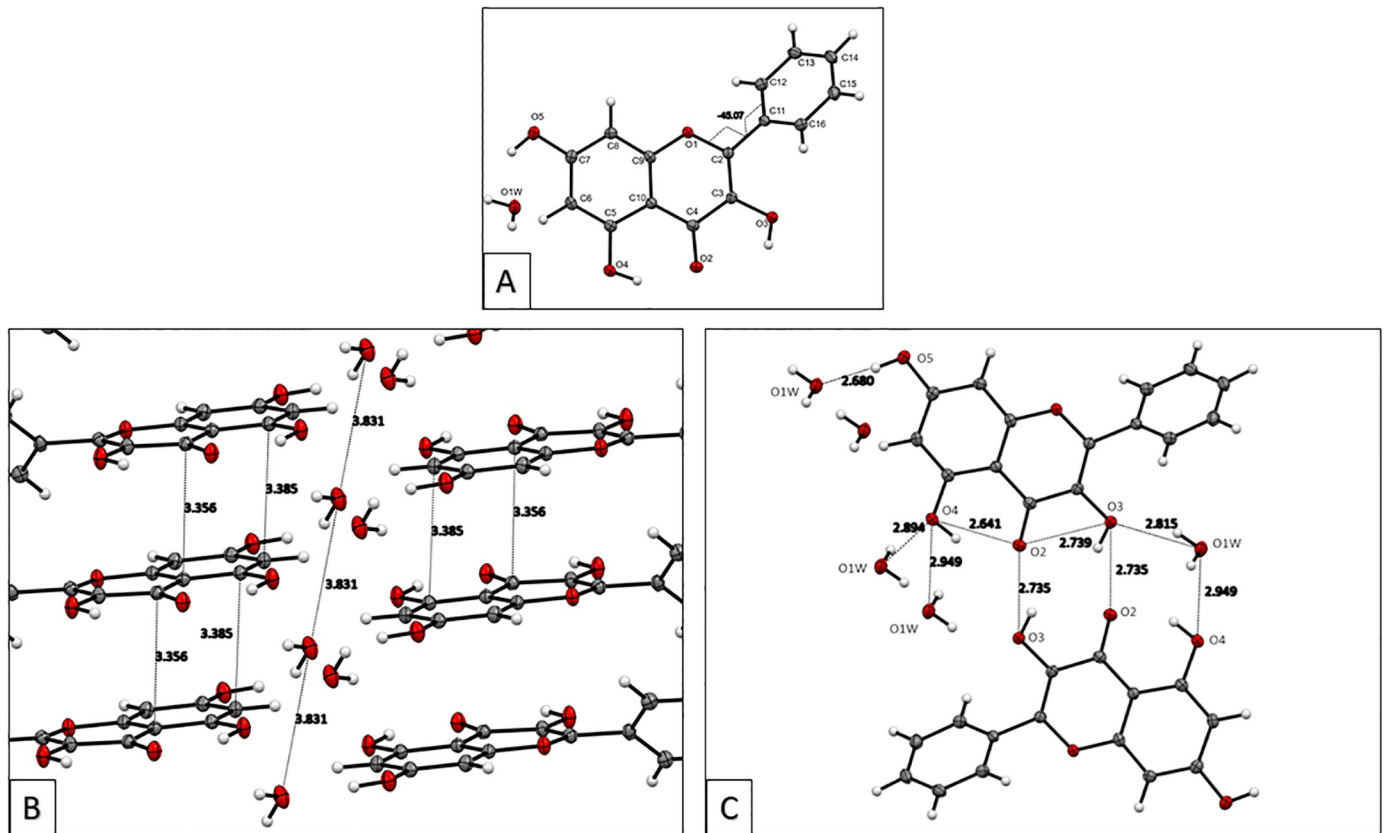
Fig 2. A: The asymmetric unit of galangin monohydrate with atom labeling and the torsion angle about the C2-C11 bond at -45.1(2°; B: Offset stacking interactions among galangin molecules (about 3.35–3.38 Å). The repeat distance between water molecules of 3.831Å is equivalent to the unit cell *a* axis length; C: Distances of hydrogen bonding interactions in the galangin crystal structure.

https://doi.org/10.1371/journal.pone.0267624.g002

scavenging the superoxide radical. As will be described later, galangin is a good scavenger of superoxide and here we propose a potential mechanism of scavenging. The common mechanism by which polyphenols scavenge radicals is through H-atom transfer from a polyphenol hydroxyl to the radical. In galangin, there are 3 potential hydrogen atoms donors from the

Table 2. Hydrogen bonds for galangin [Å and °].

D-H...A	d(D-H)	d(H...A)	d(D...A)	<(DHA)
O(3)-H(3)...O(2)#1	0.84(2)	2.02(2)	2.7352(15)	143(2)
O(3)-H(3)...O(2)	0.84(2)	2.28(2)	2.7391(15)	114.5(19)
O(4)-H(4)...O(2)	0.89(2)	1.85(2)	2.6405(15)	147.2(19)
O(5)-H7...O(1W)#2	0.88(2)	1.80(2)	2.6796(15)	176(2)
O(1W)-H(1W)...O(4)#3	0.87(2)	2.05(2)	2.8938(16)	163(2)
O(1W)-H(2W)...O(3)#4	0.86(2)	2.01(2)	2.8152(17)	155(2)

Symmetry transformations used to generate equivalent atoms:

[#1] -x+1,-y+2,-z+1

[#2] x-1,y,z

[#3] -x,-y+1,-z+1

[#4] x,y-1,z

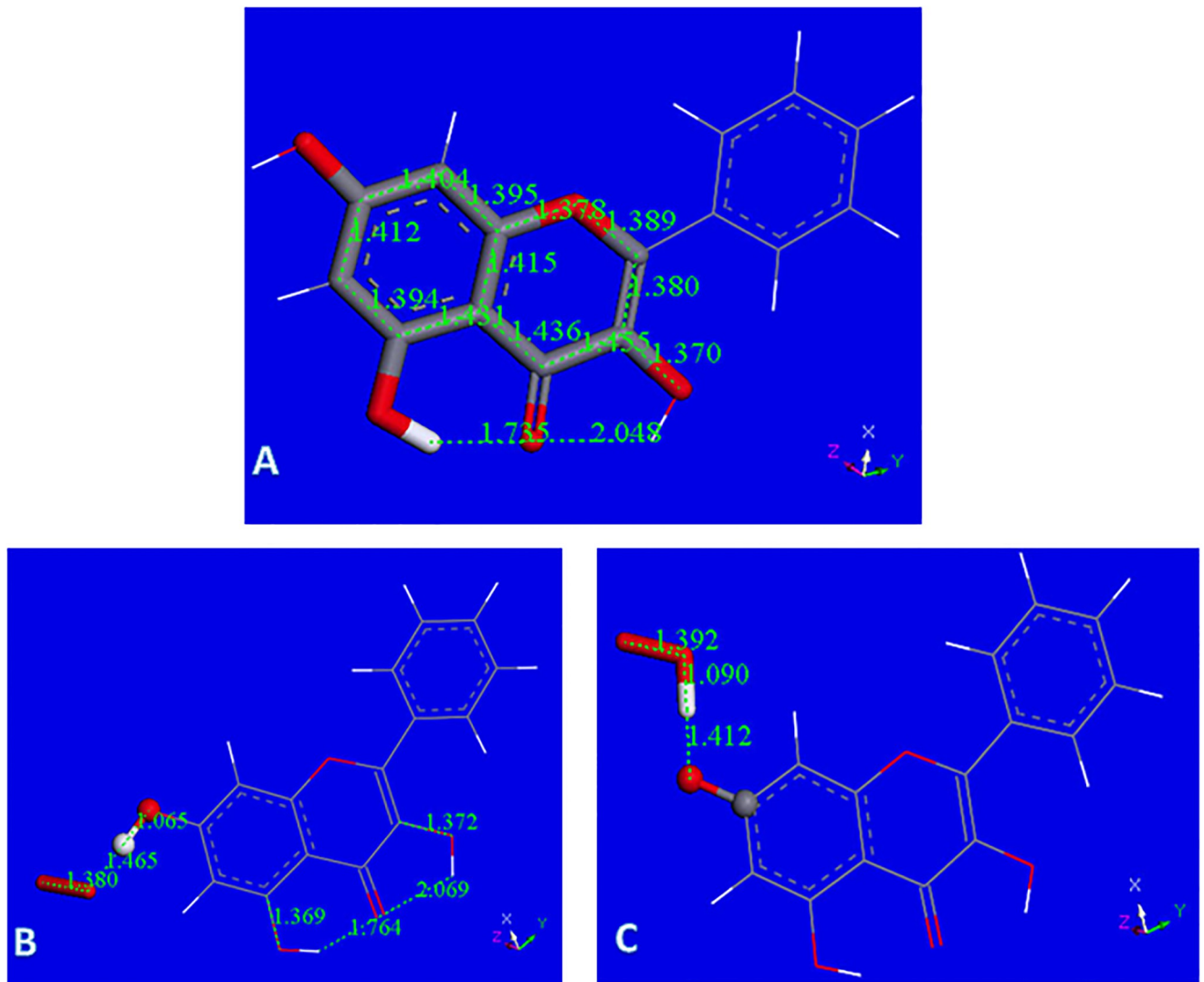https://doi.org/10.1371/journal.pone.0267624.t002

Fig 3. A: Galangin geometry obtained from X-ray coordinates after DFT minimization; B: Initial van der Waals separation between H7 and superoxide, 2.60 Å, decreases to 1.465 Å after DFT minimization, while hydroxyl separation is still a bond length, 1.065 Å. Superoxide: stick style; galangin 7-OH: ball and stick style; C: H7 was eliminated from the hydroxyl and the remaining species, the galangin radical, was DFT minimized and later placed 2.60 Å from HO_2 for further geometry minimization. Fig 3C shows the converged energy minimum: the H atom of HO_2 is not recaptured by the galangin radical, 1.412 Å. The energy of this minimum is 1.7 kcal/mol higher than that in Fig 3B, suggesting H7 of galangin is not captured by superoxide.

hydroxyl groups located in position 3, 5 and 7. Initially, one might imagine that the 7OH would be favored for this process, since the H atoms in the remaining hydroxyls of galangin form strong intramolecular H-bonds with the O(carbonyl), making these H atoms more difficult to extract from the polyphenol. Fig 3B shows the result of DFT geometry optimization for superoxide separated from H7, initially set as 2.60 Å, which is the distance corresponding to the sum of van der Waals distances for O and H atoms. It is seen that H7 is not captured by superoxide radical. However, this result may be due to an energy barrier and so we minimized the potential product to exclude that possibility: HO_2 was placed at van der Waals separation from the H7 excluded radical galangin, and the whole system becomes a radical species. This results in no recapture of H7 by the galangin radical, Fig 3C. Comparing energies of the resulting product structures shown in Fig 3C and 3B, we see that the latter is 1.7 kcal/mol lower and
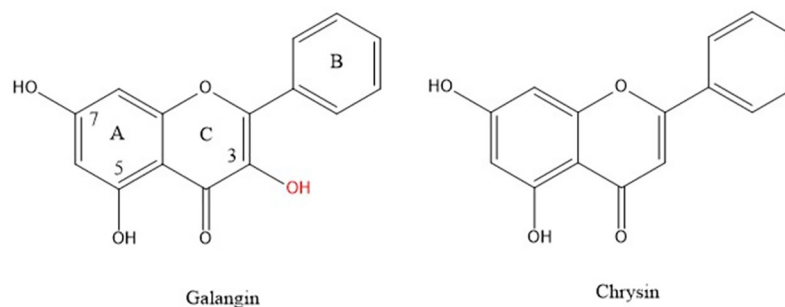
Fig 4. Galangin, 3,5,7-trihydroxyflavone, and chrysin, 5,7-dihydroxyflavone, are important components of propolis.

the positive ΔG indicates no capture of H7 by galangin. S3 Fig shows the result of geometry minimization for an initially separated proton (2.60 Å) from the O_2 moiety of Fig 3B, that results in no formation of H_2O_2. This is in contrast with the behavior of chrysin [22], where H7 was transferred to superoxide and evolved towards H_2O_2 formation. Fig 4 shows the 2D structures of galangin and chrysin. It is interesting that the presence of an additional 3-hydroxyl in galangin can preclude this type of scavenging.

However, it is known that the presence of a 3-hydroxyl in the flavonoid system induces antioxidant activity [30]. Here we show that the interaction between superoxide and this hydroxyl substituent in galangin confirms this experimental fact. Minimization of the van der Waals approached superoxide to H3(hydroxyl), Fig 5A, converges to a structure very similar to the one approaching HO_2 and the H3 excluded galangin radical, Fig 5B. More importantly, the energies of these 2 minima are exactly the same (ΔG = 0.01 kcal/mol). We conclude that the initial interaction between galangin H3 and superoxide generates a complex. It is interesting to analyze the outcome when a proton approaches this complex. From the structural complex created in the related minimization, shown in Fig 5C, it is seen that H_2O_2 is formed.

The galangin-superoxide complex shown in Fig 5A was van der Waals placed nearby a proton. This is a neutral radical that after minimization shows formation of H_2O_2 plus the galangin derivative radical, which locates the unpaired electron in the polyphenol, Fig 5C. The C3-O3 bond, 1.264 Å, becomes shorter than in galangin, (1.370 Å, Fig 3A), and very similar to the O = C4 bond, 1.265 Å. This results in rearrangement of nearby bonds: C2-C3 = 1.454 Å and C3-C4 = 1.512 Å, which are longer than in galangin 1.380 Å, and 1.455 Å, respectively, Fig 3A. C2-C1' = 1.450 Å and O1-C2 = 1.367 Å, are shorter when compared with galangin 1.473 Å and 1.389 Å, respectively in Fig 3A. Also, the aromatic B ring now shows loss of aromatization as C2'-C3' (1.394 Å) and C5'-C6' (1.396 Å), are shorter than the other C-C bonds in the ring, C1'-C2' (1.428 Å), C5'-C1' (1.426 Å). We can consider this radical having an extended conjugation. Ring A shows 2 bonds (yellow 1.390 Å and 1.399Å) shorter than lengthened bonds, (purple 1.414 Å, 1.406 Å, 1.438 Å and 1.412 Å), but this effect is already present in free galangin, Fig 3A and in the X-ray crystal structure (1.381(2) Å and 1.377(2) Å).

Using our computational results, we provide mechanistic evidence that galangin can act as a superoxide dismutase (SOD) mimic. From Fig 5C, H_2O_2 was excluded, and superoxide π-approached to ring B, which was chosen because it has some quinone characteristics and so likely to be a good target for capturing the superoxide unpaired electron. Indeed, the superoxide electron is captured by the ring, while O_2 is formed (O-O bond distance = 1.273 Å) but the latter does not penetrate galangin π system, as its separation from ring B is still similar to van
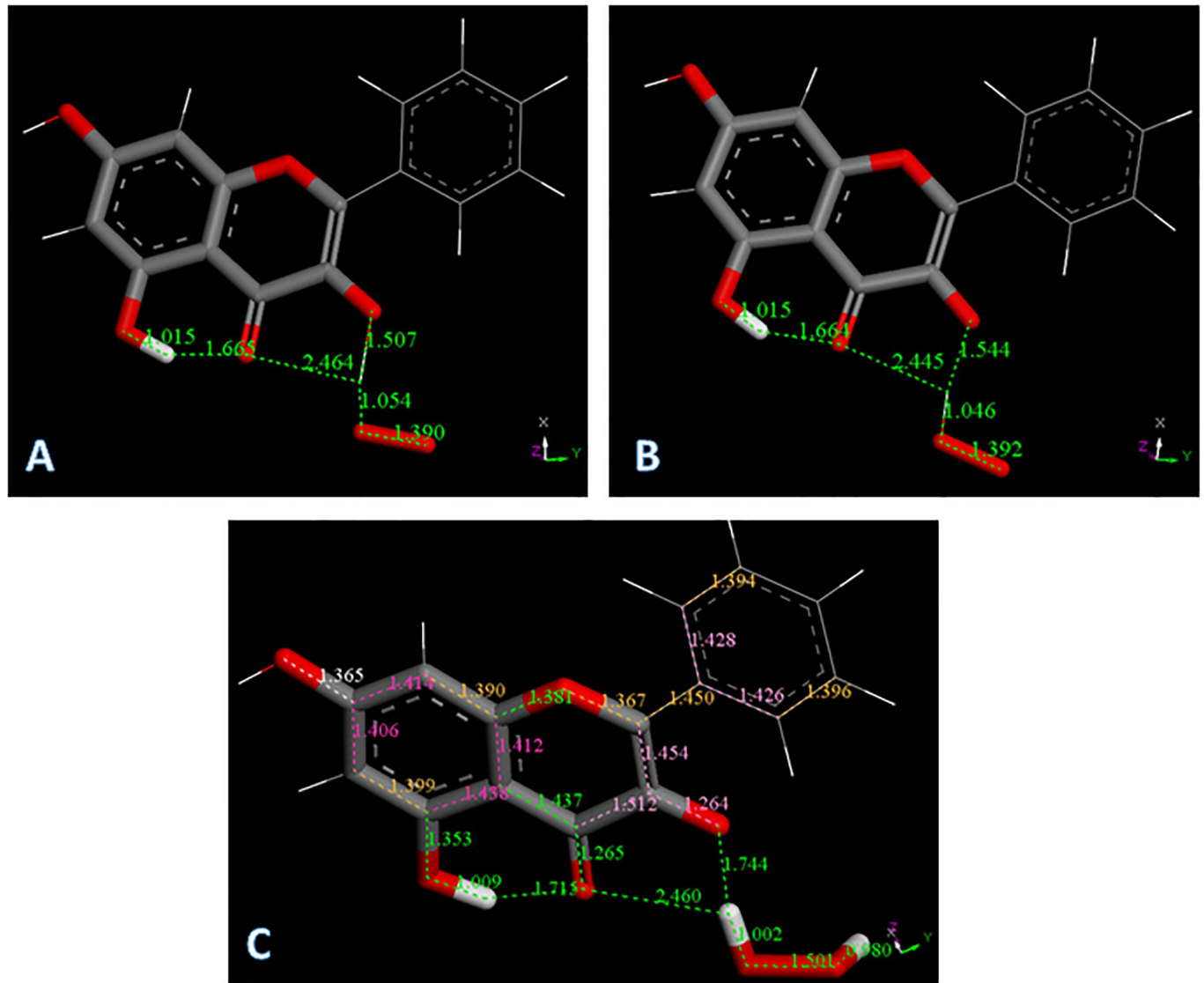
Fig 5. A: Converged DFT minimum for superoxide attack on galangin H3. The galangin O-H3 bond distance elongates to 1.507 Å and H3 advances to establish a bond distance to superoxide, 1.054 Å; B: Converged DFT minimum for initial van der Waals contact between HO_2 and the radical obtained after excluding H3 from galangin. The galangin radical does not recapture H3, 1.544 Å; C: The galangin-superoxide complex shown in Fig 5A is van der Waals placed nearby a proton. This is a neutral radical that after minimization shows formation of H_2O_2 plus the galangin derivative radical, which locates the unpaired electron in the polyphenol.

https://doi.org/10.1371/journal.pone.0267624.g005

der Waals value, 3.508 Å, Fig 6A. Hence, molecular oxygen was eliminated, and the residual structure minimized, Fig 6B. Finally, a proton was van der Waals approached to galangin O3 and, upon minimization, galangin was reformed. This suggests galangin acts as a SOD mimic for scavenging superoxide with H3 supporting reaction (a), corresponding to SOD activity:
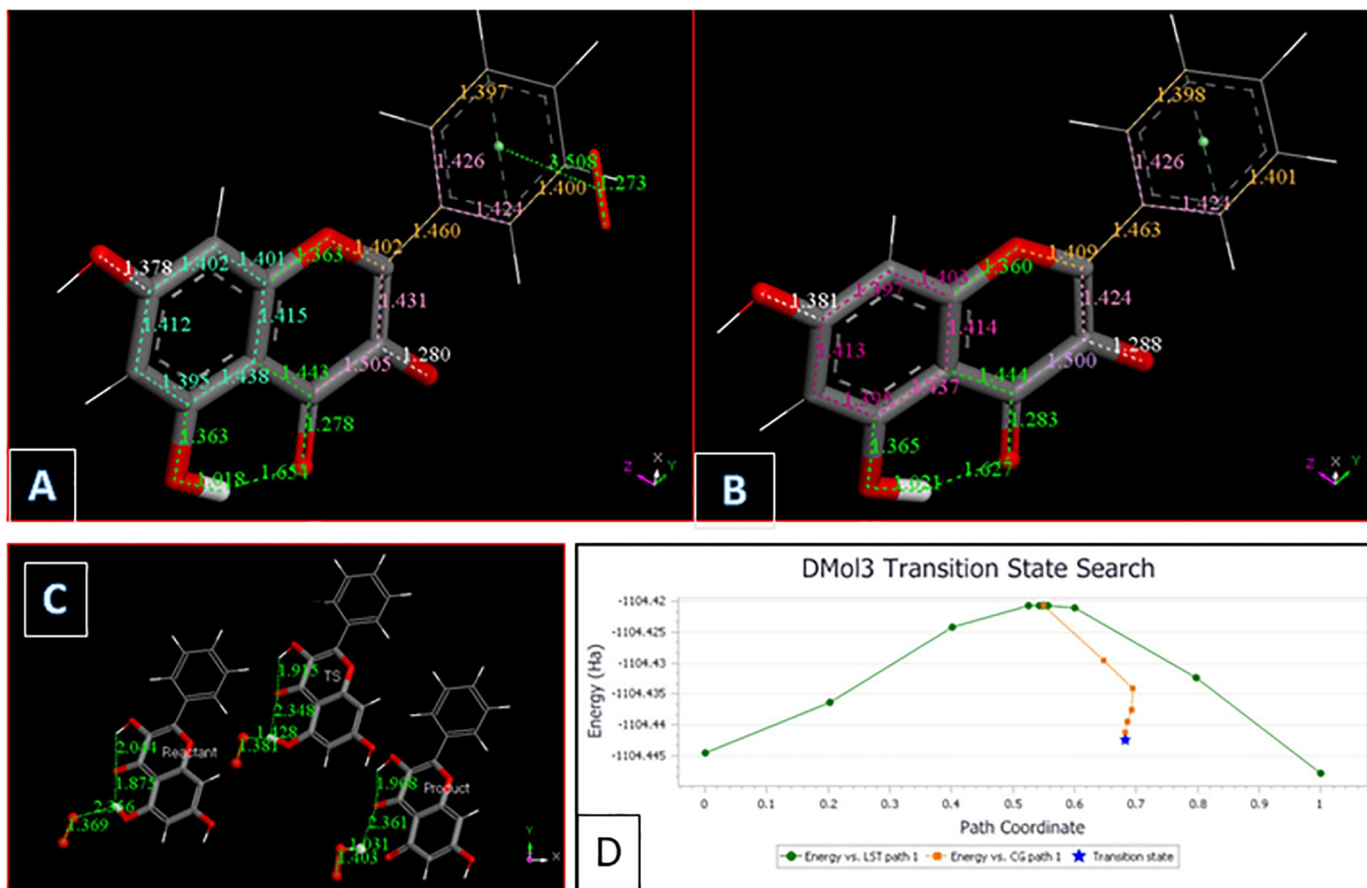
$$2\ O_2 \bullet^- + 2H^+ \rightarrow H_2O_2 + O_2 \qquad \text{(a)}$$

Fig 6. A: The π-π approach of a superoxide to galangin ring B allows for ring capture of its unpaired electron. O-O bond distance becomes similar to that in molecular oxygen, 1.273 Å, in contrast with the approached superoxide O-O, 1.373 Å. B: From previous Fig 6A O$_2$ is eliminated and DFT minimization is performed; C: Reagent, TS and Product for galangin H5 extraction by superoxide. ΔG = -2.067 kcal/mol, E(barrier) = 1.3 kcal/mol; D: TS profile for galangin H5 extraction by superoxide. ΔG = -2.067 kcal/mol, E(barrier) = 1.3 kcal/mol.

It is seen that 1) H$_2$O$_2$ is easily detached from Fig 5C, as O$_2$ is from Fig 6A, and these molecules are the products of reaction (a). In addition, after eliminating O$_2$, the arrival of a reactant proton from reaction (a), regenerates galangin, which is ready for another catalytic cycle. The second reactant proton from reaction (a) is the one added to HO$_2$ in Fig 5B and used to form H$_2$O$_2$, Fig 5C. This cycle is summarized in Scheme 1.

Scheme 1. Galangin is regenerated after reacting with 2 protons and 2 superoxide radicals. (1) Incoming superoxide (red) interacts with H3; (2) H3 is sequestered, forming HO$_2$; (3) a proton arrives and adds to HO$_2$ forming, and eliminating, H$_2$O$_2$ (light blue); (4) A second incoming superoxide (green) interacts π-π with galangin ring B; (5) the superoxide donates its electron and O$_2$ is released (light blue); (6) an incoming proton interacts with O3, re-

establishing the galangin 3OH hydroxyl group and thus reforming galangin.
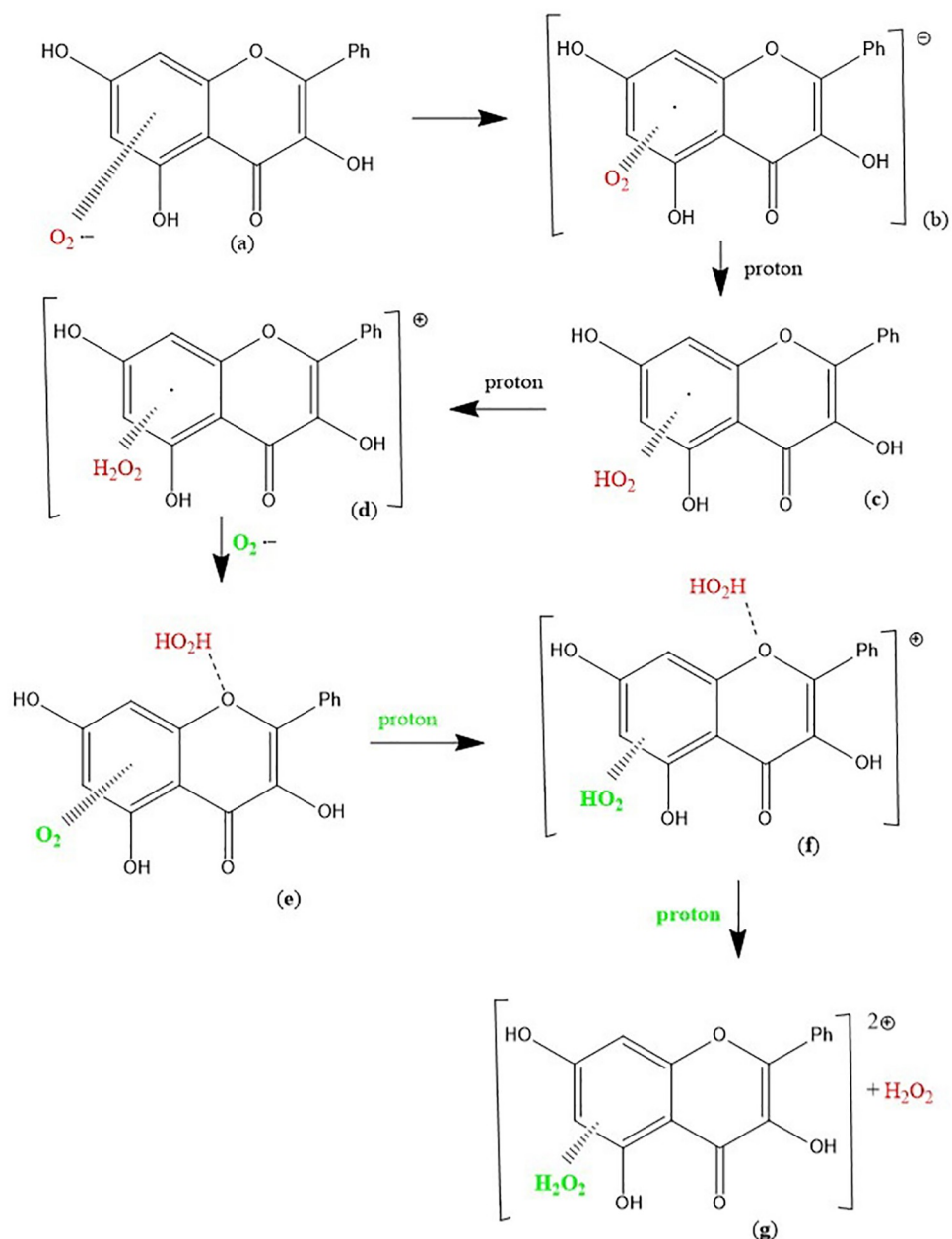
Finally, we explore if hydroxyl H5 can also detach from galangin when approached by superoxide, by performing DFT-D minimizations. Although there is some shortening between H5 and superoxide, it is much weaker than that seen for H3, and additional approach by a proton does not induce H_2O_2 formation (not shown). Hence, we studied the behavior of the potential product, which is an HO_2 moiety interacting with galangin after H5 exclusion. The energy of this product is lower and a TS was explored. Fig 6C and 6D, show that the capture of H5 by superoxide is feasible: $\Delta G = -2.067$ kcal/mol, E(barrier) = 1.3 kcal/mol.

We conclude that, abstraction of a galangin H atom by superoxide is feasible for hydroxyl hydrogens H3 and H5, with H3 slightly favored because it is a thermodynamically spontaneous
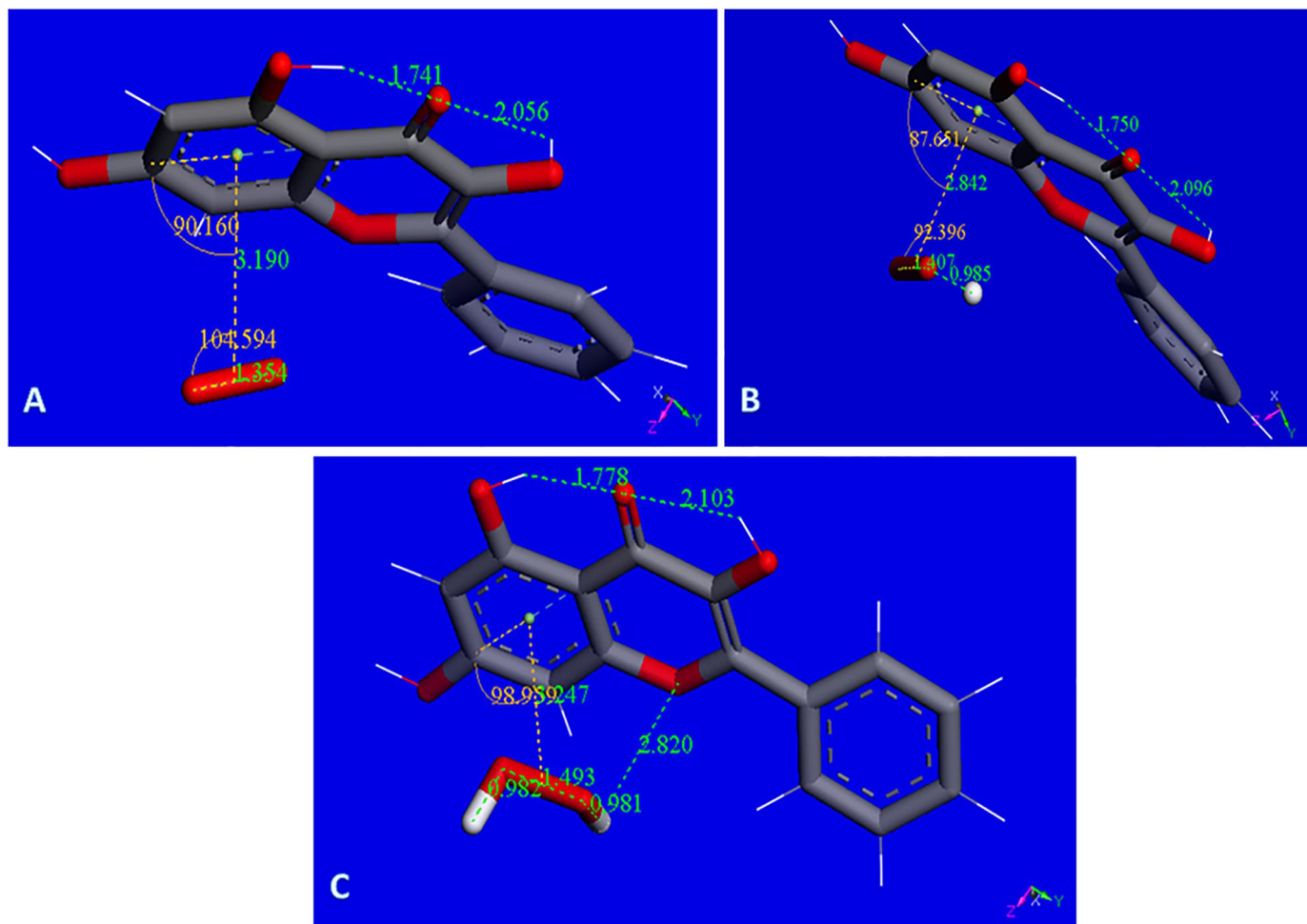
Fig 7. A: Galangin accepts a π-π approach by superoxide. Initially van der Waals separated molecules, 3.50 Å, are geometrically optimized. Both reagents become closer with centroid-centroid separation stabilized 3.190 Å apart. There is a slight shortening of O-O bond distance in superoxide, 1.354 Å, from the original 1.373 Å; B: Galangin π–π superoxide from previous Fig 7A is now approached by a proton that, after minimization, becomes stabilized by formation of an O-H bond, 0.985 Å, while superoxide O-O separation is lengthened, 1.407 Å (it was 1.354 Å in Fig 7A); C: From previous Fig 7B, an additional proton is placed 2.60 Å from HO$_2$. Upon minimization H$_2$O$_2$ is formed, however, it is in a complex with the galangin ring, as shown by the centroid-centroid separation of 3.247 Å, shorter that the 3.50 Å π–π van der Waals separation.

https://doi.org/10.1371/journal.pone.0267624.g007

process, whereas H5 needs to overcome an energy barrier. However, this H5 barrier is easily affordable (1.3 kcal/mol). Also, in contrast with chrysin [22], H7 galangin is not captured by superoxide.

The antioxidant ability of flavonoids has been studied fro some time [11–17]. Recently, computational studies on flavonoid derivatives, including galangin and quercetin, have focused primarily on the importance of hydroxyl groups in exocyclic phenyl ring B (which galangin does not have) and pyrone ring C (the C-3 hydroxyl group) present in both galangin and quercetin [18]. Our DFT results are in agreement with findings in this study, than the hydroxyl H3 atom is slightly favored for hydrogen abstraction and antioxidant activity, over hydroxyl H5.

Our previous investigations on superoxide scavenging by embelin [31] emodin [32], and chalcones [33] described an additional mode of sequestering superoxide, through the π-π interaction between superoxide radical and the polyphenol. This scavenging mechanism is suggested for galangin as well, since, as described later in RRDE results, galangin is
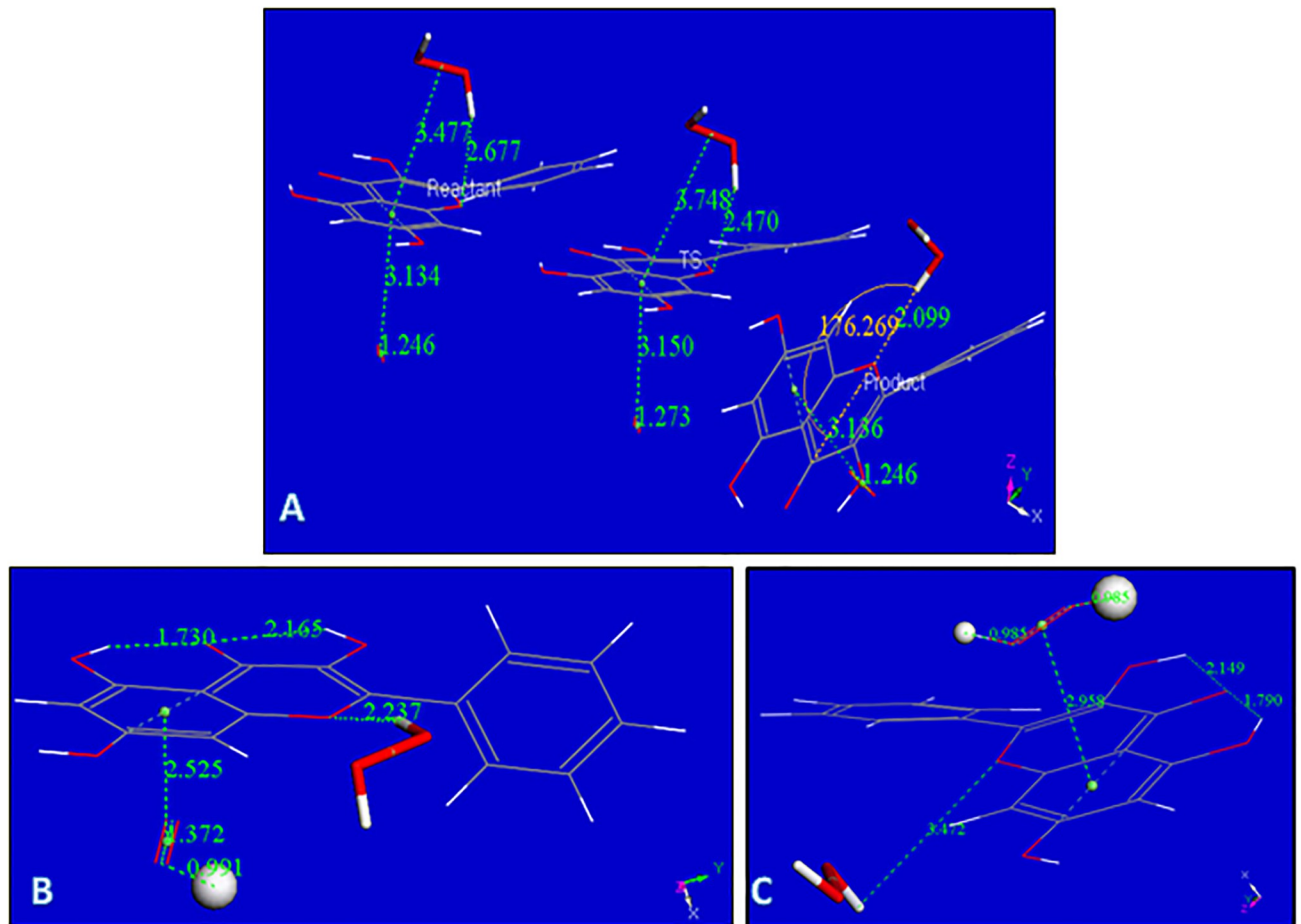
Fig 8. A: Rearrangement of H_2O_2 moiety as described by the Transition State search (TS): left, reagent; center TS; right, product, are displayed; B: From the product of Fig 8A proton is captured by the O_2 moiety, total charge is 1; C: From Fig 8B an additional proton, small ball size, is captured by the HO_2 moiety forming H_2O_2, while the other H_2O_2 located in the polyphenol plane, detaches from galangin, 3.472 Å. Total charge of this radical species is 2.

experimentally found to be an excellent scavenger of superoxide, and additional options need to be considered. Computational results seen in Fig 7A show the related minimization structure where centroid-centroid separation stabilized at 3.190 Å, from an initial van der Waals separation of 3.5 Å. The complex incorporates a proton captured by the O_2 moiety, Fig 7B, and an additional proton generates the H_2O_2 moiety, still coordinated to the polyphenol, Fig 7C. An additional calculation for interaction to a 2nd superoxide radical, entering from the opposite side of H_2O_2, (S4 Fig, the input configuration) shows the incoming group stabilized with a centroid-centroid separation of 3.134 Å. The original separation between superoxide O atoms becomes much shorter, 1.246 Å, corresponding to the expected length of a O_2 molecule, but still bound to the polyphenol. It is clear that the superoxide unpaired electron is now located within the polyphenol structure and this species is *not* a radical, as the number of electrons is now *even* due to 2 superoxides incorporated into the complex. It is noteworthy that one H from H_2O_2 now is within H-bonding distance (2.820 Å) to the polyphenol O1. To analyze the corresponding potential H_2O_2 transfer to the polyphenol plane, a transition state calculation was performed after observing that the product has lower energy than the reagent, Fig 8A and 8B.

Fig 8A includes the minimum geometry reached after minimization of S4 Fig. The H_2O_2 moiety protrudes towards ring C, with a H-bond distance between O1 (galangin) and H (H_2O_2) of 2.677 Å, suggesting a potential rearrangement. This is confirmed with a transition state search where the product is shown on the right in Fig 8A, and the corresponding TS is in center of Fig 8A. ΔG is -0.04 kcal/mol and E(barrier) of 3.9 kcal/mol. S5 Fig shows the TS energy profile.

Fig 8B shows the arrival of a proton to the O_2 moiety of the product just described. After incorporation of another proton into the HO_2 unit, a 2nd molecule of H_2O_2 is formed while the first H_2O_2, located in the polyphenol plane detaches, with O(1)- - -H(H_2O_2) separation of 3.472 Å, Fig 8C. After elimination of the first H_2O_2 molecule, it is possible to incorporate an additional superoxide, Fig 9A and 9B.

Attempts to explore if the newly formed O_2 species, trans to H_2O_2, or H_2O_2 itself, are able to detach from the Fig 9B complex failed, although additional superoxide radicals were incorporated as seen in the arrangement of Fig 9C. Indeed, the complex shown in Fig 9C contains the maximum number of superoxide radicals captured by galangin in this study. It is strongly
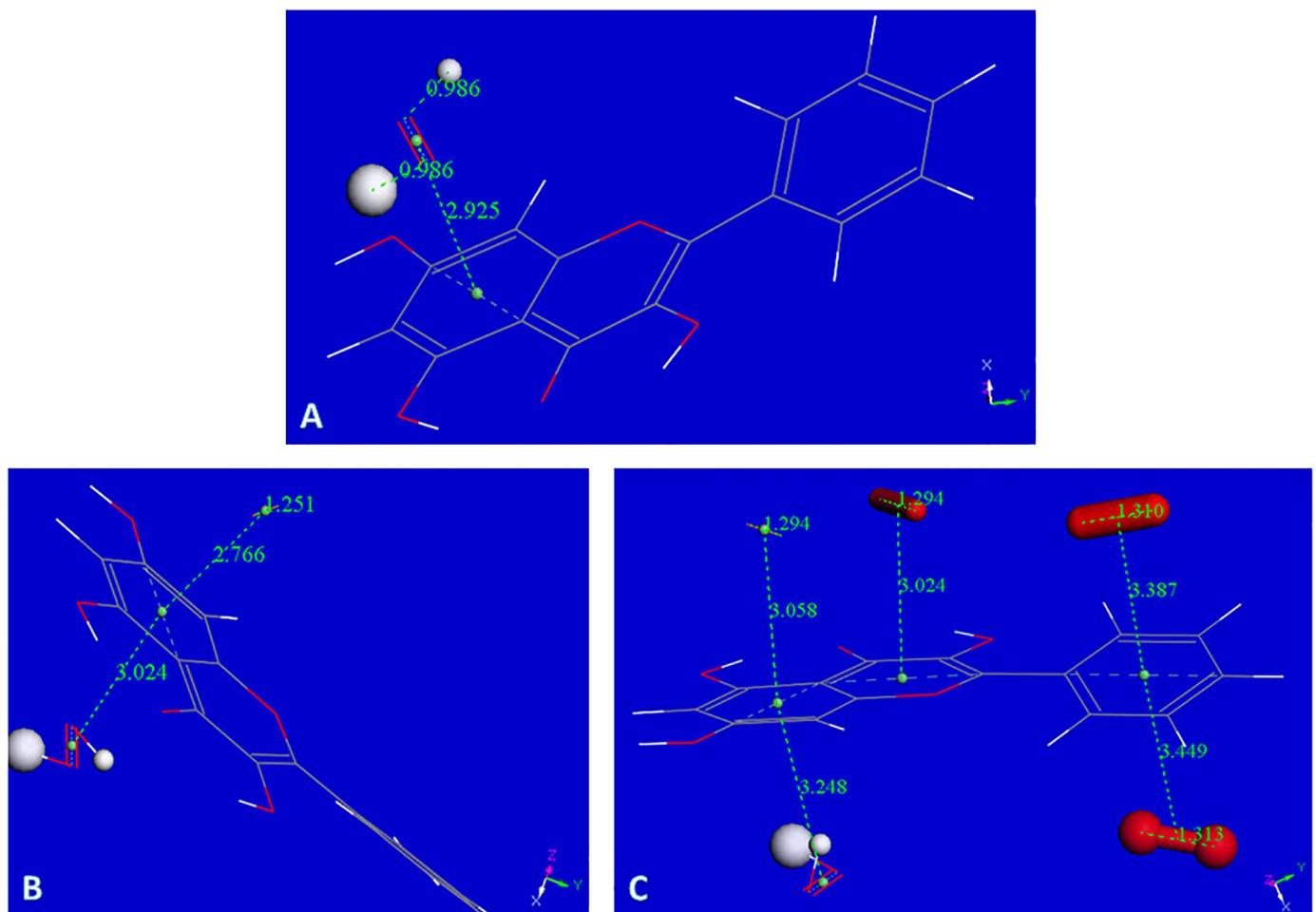

Fig 9. A: Minimum reached after excluding H_2O_2 from Fig 8C. Total charge is still 2; B: Superoxide entering trans to H_2O_2 moiety, total charge 1. This is a non-radical species and the O-O separation for the newly arrived superoxide, 1.251 Å, is much shorter than the original 1.373 Å, and similar to O-O bond length in O_2; C: After the arrangement shown in Fig 9B, three additional superoxide radicals are incorporated above and below the aromatic plane of galangin.

suspected that if additional protons are available they may be incorporated to stabilize further H_2O_2 units. This DFT study is summarized in the following Scheme 2.

Scheme 2. The π-π scavenging of superoxide by galangin: (a) Superoxide interacts with galangin ring A (π-π approach); (b) the unpaired electron enters the galangin ring; (c) (d) two protons are incorporated within the O_2 moiety forming H_2O_2; (e) a 2nd superoxide is incorporated, (f) a proton captured by O_2 forms a HO_2 moiety; (g) after an additional proton the original H_2O_2 (red) detaches from O-1 galangin position.
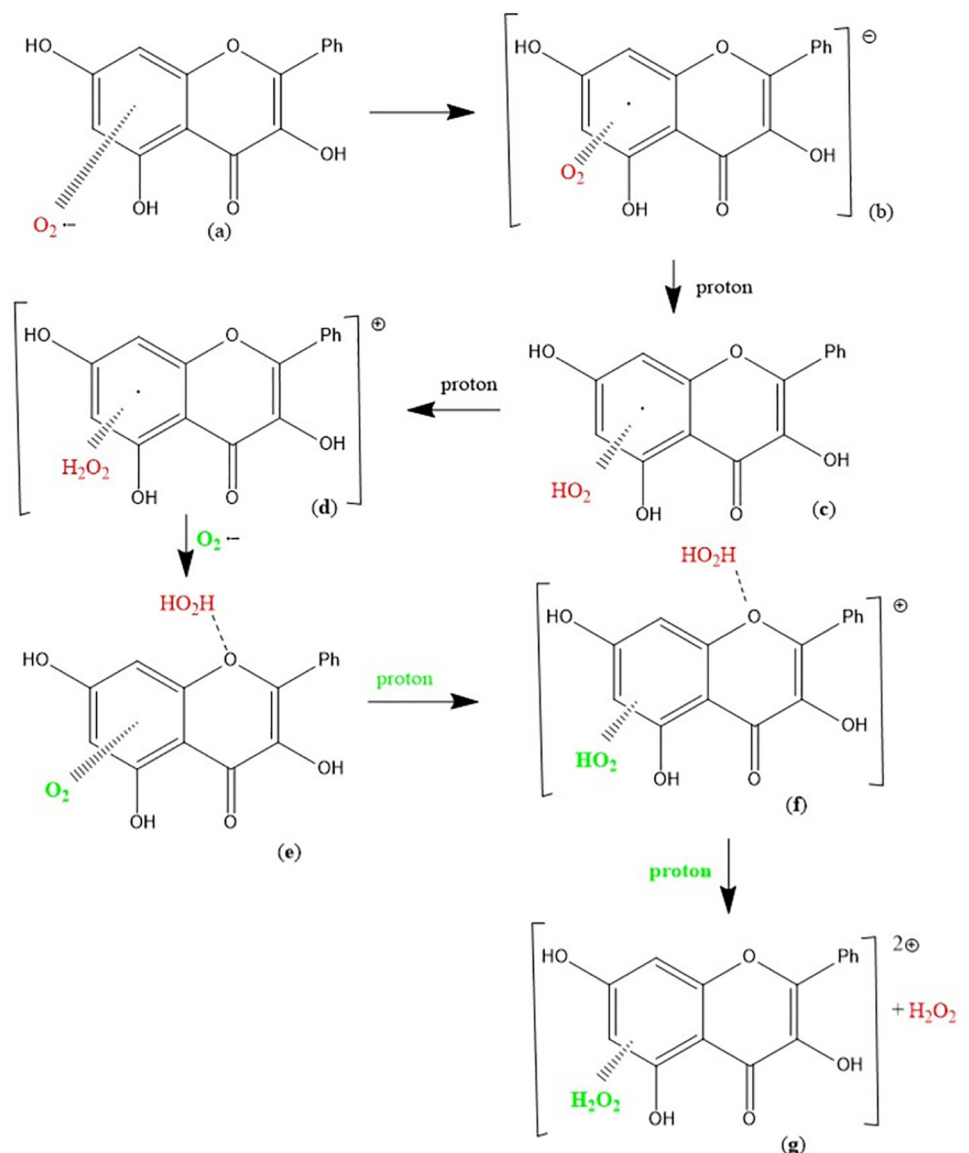
We see that the π-π approach of superoxide to galangin is favored and even 4 superoxide radicals can be stabilized along with a H_2O_2 molecule on galangin (Fig 9C), with total charge = -2, which is surprisingly high. This complex is a result of 5 incorporated superoxide and 2 protons, but before formation of this complex, H_2O_2 formation and release was described. Thus, the number of superoxide anions associated with galangin in this π-π superoxide-galangin
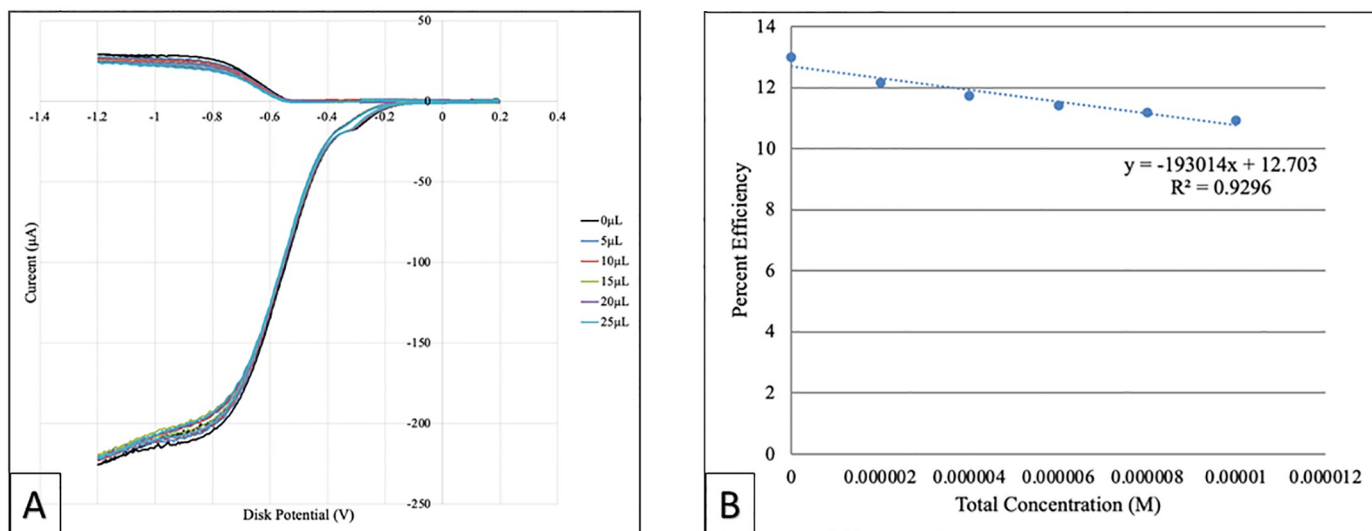
Fig 10. A: A total of 5 runs of galangin were performed in this study. This CV compilation shows the initial blank, black color, and colored aliquots added of galangin; B: Antioxidant Efficiency of galangin, as function of molarity.

study is six, which when added to 4 protons, defines the final charge of the complex (-2) shown in Fig 9C.

From this DFT study, we conclude that 1) galangin hydroxyls H3 and H5 can be captured by superoxide, suggesting galangin acts as a mimic of SOD catalysis; 2) H7 is not captured by superoxide; 3) galangin π-π interactions can incorporate several superoxide radicals, and form a detached H_2O_2 product. These conclusions are further discussed when analyzing the RRDE experimental results of galangin scavenging of superoxide, *vide infra*.

RRDE

The antioxidant activity of galangin was determined based on its superoxide radical scavenging ability that was measured using a protocol developed in our lab [22]. In this cyclic voltammetry method superoxide is developed *in situ* by bubbling O_2 into the electrovoltaic cell containing anhydrous DMSO solvent, see details in Experimental section. After the blank experiment, aliquots taken from a stock 0.02M galangin solution, were added to the voltaic cell. Fig 10A shows voltammograms of blank and all runs for both electrodes. The lower part of these voltammograms develops at the disk electrode, where O_2 incorporates an electron to generate superoxide $O_2 \bullet^-$. The opposite effect, oxidation of $O_2 \bullet^-$, takes place at the ring electrode, which has a fixed potential enough positive for this action, upper part. As scavenger aliquots are added, they consume part of the superoxide and the ring disc detects less superoxide, lowering the current. The collection efficiency is shown in Fig 10B, for all data, showing the decrease of superoxide. All scavengers studied by us so far behaved in a linear manner for the initial aliquots used. Beyond the initial aliquots, 2 possibilities were seen: (1) complete linear behavior, as in, chrysin [22], eriodictyol [22], BHT [31], emodin [32], celastrol [34] or (2) initial linear behavior followed by asymptotic performance, such as in quercetin [22], embelin [31] and clovamide [35]. In the present study, we also calculated a linear trend for all data, with regression factor of 0.9296, whereas the initial 3 data (using the blank plus 2 initial added aliquots) have a linear regression factor of 0.9635, slightly better, but still not ideal. Since we find that several superoxide anions are incorporated in one galangin unit, Fig 9C, galangin is a very efficient scavenger, and indeed this is demonstrated by the slope in Fig 10B, -19×10^4. In

fact, when comparing with previous studies following the same protocol, quercetin [31], (slope = -6.0×10^4) was the radical scavenger showing the steepest slope; in this study, galangin shows an even stronger superoxide scavenging capacity than quercetin. This is in contrast with calculations reported by Spiegel et al. [18] where thermodynamic parameters showed quercetin as a better radical scavenger, and which was explained as due to the catechol moiety present in phenyl ring B of quercetin.

Our DFT study demonstrates the strong capability of galangin to capture superoxide radicals via π-π interaction. This is in agreement with our experimental RRDE showing galangin to be a better antioxidant than quercetin by having a steeper slope (Fig 10B) compared with quercetin. It is interesting that the commercially used antioxidant, BHT, has a much milder slope, -1.6×10^3, [31].
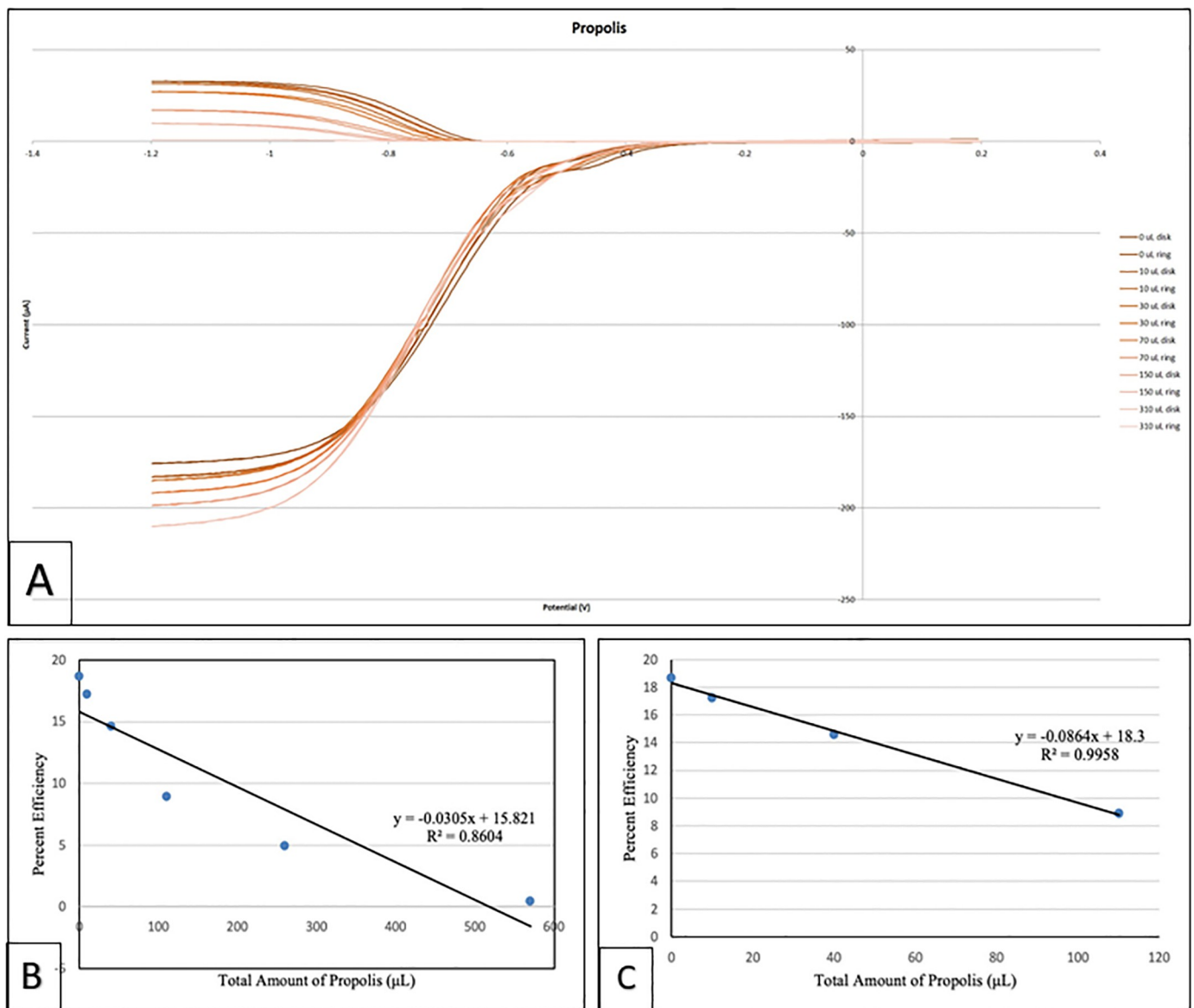

Fig 11. A: Cyclovoltammograms of propolis when scavenging the superoxide radical, B: Collection efficiency of propolis; linear behavior considering all runs. The last run shows almost complete elimination of superoxide; C: Linear behavior of propolis considering the first 4 data on Fig 11A.

Propolis was also analyzed using the RRDE method. Fig 11A shows the related voltammograms and Fig 11B shows the antioxidant efficiency of propolis when scavenging the superoxide radical where the x-axis denotes the total volume of added aliquots; the linear form shows a non-ideal regression factor, 0.8604. Fig 11C only considers the initial 4 points of Fig 11B shows a linear behavior with an excellent regression factor, 0.9958. When comparing with our previously described RRDE analysis of olive oil [36], which is also a mixed substrate, propolis shows higher antioxidant activity, as shown by an almost complete elimination of superoxide after the last aliquot.

Conclusions

Results from cyclic voltammetry using a ring disk electrode (RRDE), show that galangin is a powerful scavenger of the superoxide radical anion. This is compatible with the galangin crystal structure that shows a rich network of hydrogen bonds and stacking interactions. Using DFT methods, π-π interaction between superoxide and galangin are further confirmed; these interactions are in part responsible for superoxide oxidation and capture of the superoxide electron by the aromatic rings of galangin. Additionally, abstraction of galangin H3 and H5 by superoxide is also demonstrated and associated with SOD action by galangin. This SOD action may be responsible for the RRDE steeper slope of galangin compared with quercetin [22]. When analyzing propolis, RRDE results show very strong antioxidant capability, including almost complete elimination of superoxide from the electrochemical cell. Since propolis contains other scavengers besides galangin, a main component of propolis, the total amount of effective compounds in the propolis contribute to the antioxidant activity.

Supporting information

S1 Fig. Unit cell packing as viewed down *a*-axis, down *b*-axis and down *c*-axis, from left to right.
(JPG)

S2 Fig. Galangin unit cell offset stacking at 3.356 Å. The diagram on the right is approximately perpendicular to the view on left.
(JPG)

S3 Fig. From previous Fig 4C a proton was placed at van der Waals separation from the superoxide (2.60 Å). After geometry optimization this proton went further away, 2.890 Å. Thus, this proton does not induce H_2O_2 formation, a potential product resulting from scavenging of superoxide by polyphenols.
(TIF)

S4 Fig. In this DFT calculation, an additional superoxide is placed on the opposite side of the galangin ring A from the H_2O_2, at initial separation of 3.50 Å.
(TIF)

S5 Fig. TS profile of reaction in Fig 8A.
(TIF)

Acknowledgments

Author Contributions

Conceptualization: Miriam Rossi.

Data curation: Molly Berinato, Melissa Hernandez.

Investigation: Francesco Caruso, Christopher Smart, Miriam Rossi.

Methodology: Francesco Caruso, Stuart Belli.

Project administration: Miriam Rossi.

Resources: Christopher Smart.

Software: Melissa Hernandez.

Validation: Francesco Caruso, Stuart Belli.

Writing – original draft: Francesco Caruso, Miriam Rossi.

References

1. Zabaiou N, Fouache A, Trousson A, Baron S, Zellagui A, Lahouel M, et al. (2017) Biological properties of propolis extracts: Something new from an ancient product. Chem Phys Lipids 207 (Pt B): 214–222. https://doi.org/10.1016/j.chemphyslip.2017.04.005 PMID: 28411017

2. Wagh VD. (2013) Propolis: a wonder bees product and its pharmacological potentials. Adv Pharmacol Sci 2013: 308249. https://doi.org/10.1155/2013/308249 PMID: 24382957

3. Curti V, Zaccaria V, Sokeng AJT, Dacrema M, Masiello I, Mascaro A, et al. (2019) Bioavailability and in vivo antioxidant activity of a standardized polyphenol mixture extracted from brown propolis. Int J Mol Sci 20: 1250. https://doi.org/10.3390/ijms20051250 PMID: 30871097

4. Liang X, Wang P, Yang C, Huang F, Wu H, Shi H, et al. (2021) Galangin inhibits gastric cancer growth through enhancing STAT3 mediated ROS production. Front Pharmacol 12: 646628. https://doi.org/10.3389/fphar.2021.646628 PMID: 33981228

5. Liu D, You P, Luo Y, Yang L, Liu Y. (2018) Galangin induces apoptosis in MCF-7 human breast cancer cells through mitochondrial pathway and phosphatidylinositol 3-Kinase/Akt Inhibition. Pharmacology 102: 58–66. https://doi.org/10.1159/000489564 PMID: 29879712

6. Russo A, Longo R, Vanella A. (2002) Antioxidant activity of propolis: role of caffeic acid phenethyl ester and galangin. Fitoterapia 73: S21–S29. https://doi.org/10.1016/s0367-326x(02)00187-9 PMID: 12495706

7. Hewage SRKM, Piao MJ, Kim KC, Cha JW, Han X, Choi YH, et al. (2015) Galangin (3,5,7-trihydroxyflavone) shields human keratinocytes from ultraviolet B-induced oxidative stress. Biomol Therap 23: 165–173. https://doi.org/10.4062/biomolther.2014.130 PMID: 25767685

8. Basri AM, Taha H, Ahmad N. (2017) A review on the pharmacological activities and phytochemicals of Alpinia officinarum (Galangal) extracts derived from bioassay-guided fractionation and isolation. Pharmacogn Rev 11: 43–56. https://doi.org/10.4103/phrev.phrev_55_16 PMID: 28503054

9. Pillai MK, Young DJ, Majid HMBHA. (2018) Therapeutic potential of Alpinia officinarum. Mini Rev Med Chem 18: 1220–1232. https://doi.org/10.2174/1389557517666171002154123 PMID: 28969549

10. Dorta DJ, Pigoso AA, Mingatto FE, Rodrigues T, Prado IMR, Helena AFC, et al. (2005) The interaction of flavonoids with mitochondria: Effects on energetic processes. Chem Biol Interact 152: 67–78. https://doi.org/10.1016/j.cbi.2005.02.004 PMID: 15840381

11. de Souza GLC, Peterson KAJ. (2021) Benchmarking Antioxidant-Related Properties for Gallic Acid through the Use of DFT, MP2, CCSD, and CCSD(T) Approaches. Phys Chem A 125: 198–208. https://doi.org/10.1021/acs.jpca.0c09116 PMID: 33400511

12. Mendes RA, Almeida SKC, Soares IN, Cristina A, Barboza A, Freitas RG, et al. (2019) Evaluation of the antioxidant potential of myricetin 3-*O-α-L*-rhamnopyranoside and myricetin 4′-*O-α-L*-rhamnopyranoside through a computational study. J Mol Model 25: 89. https://doi.org/10.1007/s00894-019-3959-x PMID: 30847605

13. Rong YZ, Wang ZW, Zhao B. (2013) DFT-Based Quantum Chemical Studies on Conformational, Electronic and Antioxidant Properties of Isobavachalcone and 4-Hydroxyderricin. Food Byophys 8: 250–255. https://doi.org/10.1007/s11483-013-9296-1

14. Álvarez-Diduk R, Ramírez-Silva MT, Arben Merkoçi AG. (2013) Deprotonation Mechanism and Acidity Constants in Aqueous Solution of Flavonols: a Combined Experimental and Theoretical Study. J Phys Chem B 117: 12347–12359 https://doi.org/10.1021/jp4049617 PMID: 24063416

15. Sulaiman GM. (2016) Molecular structure and anti-proliferative effect of galangin in HCT-116 cells: *In vitro* study. Food Sci Biotech 25: 247–252. https://doi.org/10.1007/s10068-016-0036-4 PMID: 30263264

16. Vargas-Sanchez RD, Mendoza-Wilson AM, Torrescano-Urrutia GR, Sanchez-Escalante A. (2015) Anti-radical potential of phenolic compounds fingerprints of propolis extracts: DFT approach. Comput Theor Chem 1066: 7–13. https://doi.org/10.1016/j.comptc.2015.05.003

17. Kozlowski D, Marsal P, Steel M, Mokrini R, Duroux J-L, Lazzaroni R, et al. (2007) Theoretical Investigation of the Formation of a New Series of Antioxidant Depsides from the Radiolysis of Flavonoid Compounds. *Radiat Res* 168: 243–252. https://doi.org/10.1667/RR0824.1 PMID: 17638407

18. Spiegel M, Andruniów T, Sroka Z. (2020) Flavones' and flavonols' antiradical structure–activity relationship. A quantum chemical study. Antioxidants 9: 461. https://doi.org/10.3390/antiox9060461 PMID: 32471289

19. Sheldrick GM. (2015) Crystal structure refinement with SHELXL. Acta Crystallogr C71, 3–8. https://doi.org/http%3A//dx.doi.org/10.1107/S2053229614024218 PMID: 25567568

20. Macrae CF, Sovago I, Cottrell SJ, Galek PTA, McCabe P, Pidcock E, et al. (2020) Mercury 4.0: from visualization to analysis, design and prediction. J Appl Crystallogr 53 (Pt 1): 226–235. https://doi.org/10.1107/S1600576719014092 PMID: 32047413

21. Mayrhofer KJJ, Strmcnik D, Blizanac BB, Stamenkovic V, Arenz M, Markovic NM. (2008) Measurement of oxygen reduction activities via the rotating disc electrode method: From Pt model surfaces to carbon-supported high surface area catalysts Electrochim Acta 53: 3181–3188. https://doi.org/10.1016/j.electacta.2007.11.057

22. Belli S, Rossi M, Molasky N, Middleton L, Caldwell C, Bartow-McKenney C, et al. (2019) Effective and novel application of hydrodynamic voltammetry to the study of superoxide radical scavenging by natural phenolic antioxidants. Antioxidants. 8: 14. https://doi.org/10.3390/antiox8010014 PMID: 30621138

23. Delley BJ. From molecules to solids with the DMol3 approach. (2000) J Chem Phys 113: 7756–7764. https://doi.org/10.1063/1.1316015

24. Perdew JP, Chevary JA, Vosko SH, Jackson KA, Pederson MR, Singh DJ, et al. (1992) Atoms, molecules, solids, and surfaces: Applications of the generalized gradient approximation for exchange and correlation. Phys Rev B Cond Mat Mater Phys 46: 6671–6687. https://doi.org/10.1103/physrevb.46.6671 PMID: 10002368

25. Becke AD. (1988) Density-functional exchange-energy approximation with correct asymptotic behavior. Phys Rev A 38: 3098–3100, https://doi.org/10.1103/physreva.38.3098 PMID: 9900728

26. Grimme S. (2006) Semiempirical GGA-type density functional constructed with a long-range dispersion correction. J Comput Chem. 27:1787–1799. https://doi.org/10.1002/jcc.20495 PMID: 16955487

27. Lee C, Yang W, Parr RG. (1988) Development of the Colle-Salvetti correlation-energy formula into a functional of the electron density. Phys Rev B 37: 785–789. https://doi.org/10.1103/physrevb.37.785 PMID: 9944570

28. Groom CR, Bruno IJ, Lightfoot MP, Ward SC. (2016) The Cambridge Structural Database. Acta Crystallogr B 72: 171–179. https://doi.org/10.1107/S2052520616003954 PMID: 27048719

29. Zheng C-D, Li G, Li H-Q, Xu X-J, Gao J-M, Zhang A-L. (2010) DPPH-scavenging activities and structure-activity relationships of phenolic compounds. Nat Prod Commun 5: 1759–1765. PMID: 21213975

30. Di Meo F, Lemaur V, Cornil J, Lazzaroni R, Duroux J-L, Olivier Y, et al. (2013) Free radical scavenging by natural polyphenols: Atom versus electron transfer J Phys Chem A 117: 2082–2092. https://doi.org/10.1021/jp3116319 PMID: 23418927

31. Caruso F, Rossi M, Kaur S, Garcia-Villar E, Molasky N, Belli S, et al. (2020) Antioxidant properties of embelin in cell culture. Electrochemistry and theoretical mechanism of scavenging. Potential scavenging of superoxide radical through the cell membrane. Antioxidants 9: 382. https://doi.org/10.3390/antiox9050382 PMID: 32380755

32. Rossi M, Wen K, Caruso F, Belli S. (2020) Emodin scavenging of superoxide radical includes π–π interaction. X-ray crystal structure, hydrodynamic voltammetry and theoretical studies. Antioxidants 9: 194, https://doi.org/10.3390/antiox9030194 PMID: 32106621

33. Okoye I, Yu S, Caruso F, Rossi M. (2021) X-ray structure determination, antioxidant voltammetry studies of butein and 2',4'-dihydroxy-3,4-dimethoxychalcone. Computational studies of 4 structurally related 2',4'-diOH chalcones to examine their antimalarial activity by binding to Falcipain-2. Molecules 26: 6511. https://doi.org/10.3390/molecules26216511 PMID: 34770920

34. Caruso F, Singh M, Belli S, Berinato M, Rossi M. (2020) Interrelated mechanism by which the methide quinone celastrol, Obtained from the roots of *Tripterygium wilfordii*, inhibits main protease 3CL[pro] of COVID-19 and acts as superoxide radical scavenger. Int J Molec Sci 21: 9266. https://doi.org/10.3390/ijms21239266 PMID: 33291769

35. Ye N, Belli S, Caruso F, Roy G, Rossi M. (2021) Antioxidant studies by hydrodynamic voltammetry and DFT, quantitative analyses by HPLC-DAD of clovamide, a natural phenolic compound found in Theobroma Cacao L. beans. Food Chem 341(Pt 2): 128260. https://doi.org/10.1016/j.foodchem.2020.128260 PMID: 33039740

36. Rossi M, Caruso F, Kwok L, Lee G, Caruso A, Gionfra F, et al. (2017) Protection by extra virgin olive oil against oxidative stress in vitro and in vivo. Chemical and biological studies on the health benefits due to a major component of the Mediterranean diet. Plos One 12: e0189341. https://doi.org/10.1371/journal.pone.0189341 PMID: 29283995